*Environ. Sci. Technol.* **2007**, *41,* 5342−5348

# Continuous Analysis of Dissolved Gaseous Mercury and Mercury Volatilization in the Upper St. Lawrence River: Exploring Temporal Relationships and UV Attenuation

O'DRISCOLL, N. J.,*,† POISSANT, L.,‡ CANÁRIO, J.,§ RIDAL, J.,⊥ AND D. R. S. LEAN||

*Department of Earth and Environmental Science, Acadia University, Wolfville, Nova Scotia, B4P 2R6, Centre St-Laurent, Aquatic Ecosystem Protection Research Division, Water Science and Technology Directorate Science and Technology Branch, Environment Canada, 105 rue McGill, 7e étage (Youville) H2Y 2E7, Canada, National Institute for Fisheries and Sea Research, IPIMAR, Av. Brasilia, 1449006 Lisboa, Portugal, St. Lawrence River Institute of Environmental Sciences, Cornwall, Ontario, Canada, and Biology Department, Faculty of Science, University of Ottawa, P.O. Box 450, Stn. A., Ottawa, ON, Canada, K1N 6N5*

The formation and volatilization of dissolved gaseous mercury (DGM) is an important mechanism by which freshwaters may naturally reduce their mercury burden. Continuous analysis of surface water for diurnal trends in DGM concentration (ranging from 0 to 60.4 pg $L^{-1}$; $n$ = 613), mercury volatilization (ranging from 0.2 to 1.1 ng $m^{-2}$ $h^{-1}$; $n$ = 584), and a suite of physical and chemical measurements were performed during a 68 h period in the St. Lawrence River near Cornwall (Ontario, Canada) to examine the temporal relationships governing mercury volatilization. No lag-time was observed between net radiation and DGM concentrations (highest cross-correlation of 0.817), thus supporting previous research indicating faster photoreduction kinetics in rivers as compared to lakes. A significant lag-time (55−145 min; maximum correlation = 0.625) was observed between DGM formation and mercury volatilization, which is similar to surface water Eddy diffusion times of 42−132 min previously measured in the St. Lawrence River. A depth-integrated DGM model was developed using the diffuse integrated vertical attenuation coefficients for UVA and UVB ($K_{dl\ UVA}$ = 1.45 $m^{-1}$ and $K_{dl\ UVB}$ = 3.20 $m^{-1}$). Low attenuation of solar radiation was attributed to low concentrations of dissolved organic carbon (mean = 2.58 mg $L^{-1}$) and particulate organic carbon (mean = 0.58 mg $L^{-1}$) in the St. Lawrence River. The depth-integrated DGM model developed found that the top 0.3 m of the water column accounted for only 26% of the total depth-integrated DGM. A comparison with volatilization data indicated that a large portion (76% or 10.5 ng $m^{-2}$) of the maximum depth-integrated DGM (13.8 ng $m^{-2}$) is volatilized over a 24 h period. Therefore, at least 50% of all DGM volatilized was produced at depths below 0.3 m. These results highlight the importance of solar attenuation in regulating DGM formation with depth. The results also demonstrate both the fast formation of DGM in rivers and the importance of understanding DGM dynamics with depth as opposed to surface waters.

* Correspondingauthore-mail: Nelson.ODriscoll@ns.sympatico.ca or nelson.odriscoll@acadiau.ca.
† Acadia University.
‡ Environment Canada.
§ National Institute for Fisheries and Sea Research.
⊥ St. Lawrence River Institute of Environmental Sciences.
|| University of Ottawa.

## Introduction

Dissolved gaseous mercury (DGM), is the principal volatile form of mercury found in freshwaters. The formation and volatilization of DGM from freshwaters is important, as it is a mechanism by which water bodies may naturally reduce their mercury burden. Several studies have demonstrated that volatilization of DGM can be a substantial portion of a freshwater mercury mass budget. O'Driscoll et al. (*1*) found that the annual mass of mercury volatilized from Big Dam West Lake was equivalent to 47% of mercury inputs from wet deposition over the entire catchment area. Recent work by the METALLICUS research network has identified that 33−59% of mercury deposited in precipitation directly to a lake is quickly revolatilized over an 8 week period (*2*, *3*). Gao et al. (*4*) observed 57% of total losses in Lake Champlain were due to volatilization.

While DGM production is known to be an important aspect of the mercury cycle we have only recently begun to clarify the mechanisms and factors controlling its production and distribution. Previous work has demonstrated that DGM can be formed from a number of abiotic (*5*) and microbial (*6*) reduction processes, many of which are mediated by solar radiation. Amyot et al. (*5*) found that UVB radiation is particularly important for mercury photoreduction in low DOC temperate lakes. Other researchers have since identified UV radiation as the principal driver of DGM production in freshwaters (*7*, *8*). Therefore, the attenuation of ultraviolet radiation with depth is a key factor in mercury photoreduction through the water column.

The vast majority of published DGM values in freshwaters are for surface water (generally the top 0.3 m or less); therefore, very little is known about its formation at depths greater than 0.3 m and the resulting effects on volatilization. The limited numbers of published depth profiles for DGM in freshwaters have identified surface water as an important zone for mercury reduction (*9*); however, large increases in DGM have also been observed in very deep areas of the water column. For example, Siciliano et al. (*9*) measured increases in DGM concentration at approximately 100 m depth in the water column of Lake Ontario. Similar increases in DGM with depth have been measured in Lake Ontario (*10*) and Lake Erie (*5*). Microbial mercury reduction has been suggested as the source of DGM at depths where no solar radiation is penetrating. Siciliano et al. (*9*) found that concurrent analysis of microbial enzyme activity in Lake Ontario depth profiles showed a good correlation with DGM concentrations, which suggests a microbial reduction mechanism. Recent work has also suggested that elevated DGM concentrations in the dark hypolimnion of lakes may be regulated by the intensity and duration of phytoplankton blooms (*11*).

Solar radiation is thought to be the primary instigator of mercury reduction in most lakes and rivers (*12*). However, until the recent advent of continuous analysis methodology, the temporal resolution of DGM sampling was insufficient to analyze the temporal relationships between changes in solar radiation and DGM production. With current tech-


10.1021/es070147r CCC: $37.00 
Published on Web 07/04/2007

nologies, however, continuous analysis can be used to probe the sequence of events in contaminant photochemistry and suggest areas where mechanisms are poorly understood. O'Driscoll et al. (*13*) continuously measured DGM, mercury volatilization, and a suite of other variables during a 48 h period for two freshwater lakes in Kejimkujik Park, Nova Scotia. Using cross-correlation analysis, lag-times of 65 and 90 min were observed between incident net solar radiation and the resulting DGM formation in surface waters. The observation of a lag-time between solar radiation and DGM production in freshwater lakes is in agreement with recent work which has identified slower rate constants for gross mercury photoreduction in lakes as compared to rivers (*8*). However, the temporal relationship between DGM production and the resultant volatilization in the Kejimkujik dataset could not be analyzed due to insufficient resolution of the mercury volatilization data.

Our previous research found faster photoreduction kinetics in rivers as compared to lakes. Following this work, we test the hypothesis that there is negligible lag-time between solar radiation and DGM formation in the St. Lawrence River. The St. Lawrence River is known to contain low concentrations of dissolved organic carbon (DOC) and total suspended solids (TSS). Low attenuation of ultraviolet radiation (resulting from low DOC and TSS) may allow for substantial DGM production with depth. Therefore, we predict that a lag-time will exist between DGM formation and mercury volatilization from surface water (due to diffusion from depth). In the present work, we use continuous analysis data for DGM and mercury volatilization, as well as measurements of solar attenuation with depth collected from the St. Lawrence River to examine temporal trends in mercury reduction and subsequent volatilization. Our overall goal was to produce a depth-integrated model to accurately describe DGM production in the St. Lawrence River and to examine the relationships with mercury volatilization.

## Experimental Section

The experimental site was located on the North shore of the St. Lawrence River in Cornwall, Ontario, Canada (45°01′21.3″ north; 74°41′14.3″ west; see Supporting Information Figure SI-1). The sampling and experiments were performed over a 3-day period from May 24 to May 27, 2005 (~68 h of continuous measurements). A wooden dock extending approximately 15 meters into the river was used as a platform for the experimental equipment and the majority of the analysis was performed on site.

Water-to-air volatilization of mercury was measured using a floating Teflon dynamic flux chamber technique with a Tekran continuous gaseous mercury monitoring equipment as described by Poissant and Casimir (*14*) and Poissant et al. (*15*, *16*). The chamber consists of a hemispheric stainless steel bowl coated with Teflon. The open area of the chamber (A) is 0.125 $m^2$ and its volume is 0.010 $m^3$ (chamber is 20 cm in height). This chamber was previously intercompared with other types of flux chambers during an international study conducted in Reno, Nevada (*15*, *17*). Following Xiao et al. (*18*), the mercury flux (ng $m^{-2}$ $h^{-1}$) from the dynamic flux chamber is computed as follows:

$$F_{\mathrm{Hg}} = \frac{[\mathrm{Hg}]_o - [\mathrm{Hg}]_i}{A} \times Q \qquad (1)$$

Where: $[Hg]_o$ is the outlet air concentration; $[Hg]_i$ is the inlet air concentration into the chamber; and $Q$ is the flow rate into the chamber (0.09 $m^3$ $h^{-1}$).

The inlet measurements were made by measuring total gaseous mercury (TGM) concentrations in the ambient air at approximately 0.15 m from the chamber and from a height of ~0.10 m. Sampled air was transported to the Tekran analyzer located inside the tent shelter via a 15 m heated Teflon tubing line. Each TGM measurement was integrated over 5 min. The time resolution for the volatilization measurement was 5 min integrated. Each TGM inlet and outlet measurement was used in two separate calculations to achieve a 5-minute volatilization resolution. As such, the appropriate inlet and outlet measurements adjacent to the 5 min sampling time were used in the calculation. By doing this a 5 min resolution for mercury volatilization (flux) as opposed to a 10 or 20 min resolution was obtained. Before deploying the chamber, blanks were determined in the laboratory over an ultra clean Teflon surface. After several flushings with mercury-free air, the laboratory blanks reached the instrumental lowest blank level (2% precision of the Tekran instrument) ~0.04 ng $m^2$ $h^{-1}$. After blank determinations, the flux chamber was sealed with an ultra-clean Teflon plate and further protected within a clean plastic bag. Once at the sampling site, the bag and plate were removed and the chamber deployed on the water. The chamber was secured to a buoy at the air−water interface, as described in Poissant and Casimir (*14*) at about 90 m from the shore and above ~3 m water depth. The buoy kept the chamber at the water−air interface as well in addition to playing the role of a wave reflector. Since flow in the main channel of the St. Lawrence River is between 0.2 and 1.5 m $s^{-1}$ (*19*), we assume the near shore area is on the lower end of this flow rate. Hence it is assumed that turbulence was minimal.

Continuous analysis of dissolved gaseous mercury (DGM) was performed using the technique described by O'Driscoll et al. (*20*). St. Lawrence River water was sampled from the top 0.05 m of the water column using $^1/_4$ inch Teflon tubing attached to the floating Teflon flux chamber similar to that of O'Driscoll et al. (*13*). The Teflon sample tubing was ~1.2 m below the surface of the water until it reached the floating dock to sunlight over a 1 m interval between the tent and shoreline. Examining the attenuation of radiation in the St. Lawrence River, it was estimated that the tubing was exposed to <10% of the surface incident radiation for <3 min while in transport to the analyzer. The water was initially analyzed for pH, conductivity, oxidation−reduction potential, temperature, and dissolved oxygen using a MiniSonde 4a Hydrolab in line with the DGM analysis. After the Hydrolab analysis the DGM water was continuously removed for analysis using a 1 L glass volumetric cylinder converted to a sparger (*20*). When in continuous mode, water was pumped (using a two channel peristaltic pump with silicone pump tubing) from the lake to the Hydrolab for analysis of water chemistry, and then to the bottom of a 1 L graduated glass sparger. Water was then pumped from the sparger at the 1 L volume mark back to the lakeshore. Using a flow rate of 50 mL $min^{-1}$ the volume of sample analyzed was 250 mL every 5 min. This flow rate and sparge time has been shown to be comparable with previous discrete analysis methods (*20*). A Tekran 1100 zero air generator was used to supply mercury-free air to the glass sparger at a rate of 1.0 L $min^{-1}$. Mercury-free air was used to sparge the sample through a coarse glass dispersion tube that was placed at the bottom of the glass sparger close to the water inlet. The DGM is carried from the sparger to the sample inlet of the Tekran 2537A and analyzed for mercury content. Each Tekran 2537A used for this study was calibrated prior to this analysis using the internal mercury permeation calibration source. The internal mercury calibration source was checked for accuracy with a standard air injection of elemental mercury using a Hamilton digital syringe and a Tekran 2505 mercury vapor calibration unit. The analysis system was allowed to warm and stabilize for a minimum of 2 h before readings were recorded for interpretation. Using this method the detection limit for DGM was 20 fmol $L^{-1}$, and the relative standard deviation (RSD) of duplicates ($n = 36$) was 4.0 ± 2.6% (*20*).

Several environmental parameters were continuously measured at the site. Air temperature ($T_{air}$) and relative humidity (RH) were measured by using HMP35 humidity/temperature probes ($T_{air}$: accuracy ± 0.2 °C; RH: accuracy ± 0.04%; Campbell Scientific) at 1.75 m height above the quay surface (which is about 1 m above the water surface). Water temperature was monitored by using a 107B probe (accuracy 0.2 °C, Campbell Scientific). Net radiation (NR) for both short wave and long wave was recorded by using a Q-7.1 net radiometer (accuracy ± 4.3%, Campbell Scientific) at 1.8 m height. Wind speed (accuracy 2%) and direction (accuracy 5%) were measured by using an R.M. Young anemometer (Young Scientific) at 2.3 m height.

Scans of spectral irradiance (280−800 nm at 2 nm intervals) between 0−1.13 m depth (0, 0.001, 0.01, 0.02, 0.04, 0.06, 0.08, 0.10, 0.12, 0.14, 0.16, 0.30, 0.46, 0.60, 0.80, 1.00, 1.13 m depths) in the water column were obtained using an Optikon OL 754 spectra-radiometer with an underwater integrating sphere and fiber optic connection cable. These scans were used to calculate the diffuse vertical attenuation of ultraviolet wavebands with depth. Diffuse integrated vertical attenuation coefficients ($K_{dI}$) for integrated bands of UVB (280−320 nm) and UVA (320−400 nm) radiation were quantified by regression analysis of the semilog plot using Beer's Law (eq 2) (*21*):

$$I_z = I_0 e^{-k_{dI} \cdot z} \quad (2)$$

Where: $I_z$ is irradiance intensity (W m$^{-2}$) at depth $z$; $K_{dI}$ is the diffuse integrated vertical attenuation coefficient (m$^{-1}$); $I_0$ is the irradiance intensity at the water surface; $z$ is depth (m).

Surface water was sampled using $^1/_4$ inch Teflon tubing attached to the floating Teflon flux chamber. Samples for total mercury and dissolved organic carbon (DOC) were taken at ∼2 h intervals (24 samples over a 2 day period for DOC, 36 samples over a 3 day period for total mercury). Field quality controls included clean sampling, duplicate samples, and field blanks. Total mercury samples were collected in polypropylene tubes (*22*) and preserved using 0.5% BrCl for subsequent analysis in a class 100 clean laboratory using cold-vapor atomic fluorescence (Tekran 2600) following United States Environmental Protection Agency 1631 standard methodology (*23*).

Samples for DOC analysis were collected in poylproylene tubes and refrigerated until analysis. DOC analysis consisted of pre-filtration with 0.45 $\mu$m GF/F glass fiber filters followed by 100 °C persulfate wet oxidation and $CO_2$ detection by infrared spectroscopy (OI Corporation Model 1010 wet oxidation TOC analyzer).

A linear regression model in SPSS 10.0 software was used to derive the relationship between UVB and DGM concentrations in surface water. The derived attenuation coefficient for UVB was incorporated using Beers law to produce a depth integrated equation for aeral DGM concentrations. The integral (see eq 5) was solved using the Simpson algorithm in MATLAB (release 14) software to determine the depth-integrated areal concentrations for several different depths.

## Results and Discussion

**Diurnal Patterns and Correlations.** During the 68-hour continuous analysis of surface water diurnal patterns were observed (Figure 1) for net radiation (ranging 0−745 W m$^{-2}$; $n$ = 641), DGM (ranging 0−60.4 pg L$^{-1}$; $n$ = 613), mercury volatilization (ranging 0.2−1.1 ng m$^{-2}$ h$^{-1}$; $n$ = 584), total gaseous mercury in air (ranging 1.5−2.3 ng m$^{-3}$; $n$ = 294), oxidation−reduction potential (ranging 314−417 mV; $n$ = 522), air temperature (8.4−19.8 °C; $n$ = 641), water temperature (10−11.3 °C; $n$ = 641), relative humidity (30−100%; $n$ = 641), and wind speed (0−8.3 m s$^{-1}$; $n$ = 641). No diurnal patterns were observed in surface water for total mercury (mean = 0.40 ng L$^{-1}$; s.d. = 0.16; $n$ = 36), dissolved organic carbon (mean = 2.57 mg L$^{-1}$; SD = 0.15; $n$ = 24), specific conductivity (mean = 279.5 mS cm$^{-1}$; SD = 5.1; $n$ = 522), pH (ranging 7.4−9.9; $n$ = 513); or dissolved oxygen (mean = 7.2; SD = 0.8; $n$ = 522).

Poissant et al. (*24*) used a vertical gradient method to measure rates of mercury volatilization ranging between 0 and 9.28 ng m$^{-2}$ h$^{-1}$ (median 2.88 ng m$^{-2}$ h$^{-1}$) on Lake Ontario and the St. Lawrence River. The rates of volatilization found during this study are within this range but slightly lower than the median value measured by Poissant et al. (*24*). The lower values are likely due to variations in meteorological variables during the sampling period. The results in this study are similar to mercury volatilization rates measured in the St. Lawrence River near St-Anicet (−0.5 vs 1.0 ng m$^{-2}$ h$^{-1}$) (*14*).

Due to the cyclical changes in concentration for many of the variables several significant Pearson correlations were observed. Mercury volatilization was significantly positively correlated ($p$ < 0.01) with total gaseous mercury in air (0.70), DGM (0.55), air temperature (0.54), wind speed (0.51), net radiation (0.60), and relative humidity (0.52).

Poissant et al. (*24*) observed that mercury volatilization was not related to solar radiation and that wind speed and Henry's law constants were the primary variables in model calculations. The lack of relationship between solar radiation and mercury volatilization observed by Poissant et al. (*24*) may in part be due to the presence of a significant lag-time between the photochemical production of DGM and its diffusion to surface waters as discussed below.

**Analysis of Lag-Time.** Cross-correlation analysis was used to investigate the lag-time between diurnal cycles of net solar radiation, DGM concentration, and mercury volatilization and as first described by O'Driscoll et al., (*13*). The highest correlation between DGM and net solar radiation (correlation = 0.817) occurred with 0 min lag-time (Figure 2) indicating that there is no significant lag-time between net solar radiation and DGM formation in the St. Lawrence River. While the maximum correlation was centered at 0 min lag-time (Figure 2), the standard error on the correlation maximum (0.047) was used to determine the range of the lag-time (−55−10 min corresponding to correlations ranging from 0.775 to 0.776). These results confirm faster rates of photoreduction in rivers as compared to lakes observed in previous controlled lab analysis (*8*). O'Driscoll et al. (*13*) found two lakes in Kejimkujik Park to have lag-times between solar radiation and DGM formation ranging from 65 to 90 min, suggesting slower photoreduction kinetics in lakes as compared to rivers in our dataset.

While the exact mechanism explaining the observed fast rates of photoreduction in rivers is not fully known, recent work has demonstrated that both dissolved organic matter (DOM) structure and concentration are key variables regulating photoreducible mercury (and the associated photoreduction rates) in freshwater systems (*25*). O'Driscoll et al. (*26*) have shown that within a specific freshwater, when DOM structure is held constant, mercury photoreduction rates increase with increasing DOM concentration due to an overall increase in the associated photoreducible mercury. Our previous work suggests that the majority of photoreducible mercury is weakly bound to carboxylic functional groups and mercury that is not available for photoreduction is strongly bound to groups such as reduced thiols (*25*). As such, both DOM concentration and DOM structure are important variables controlling rates of photoreduction in freshwaters. While both DOM and total mercury concentrations are low in the St. Lawrence River it is possible that much of the mercury present may be available for photoreduction if we assume the DOM structure has fewer strong binding sites.

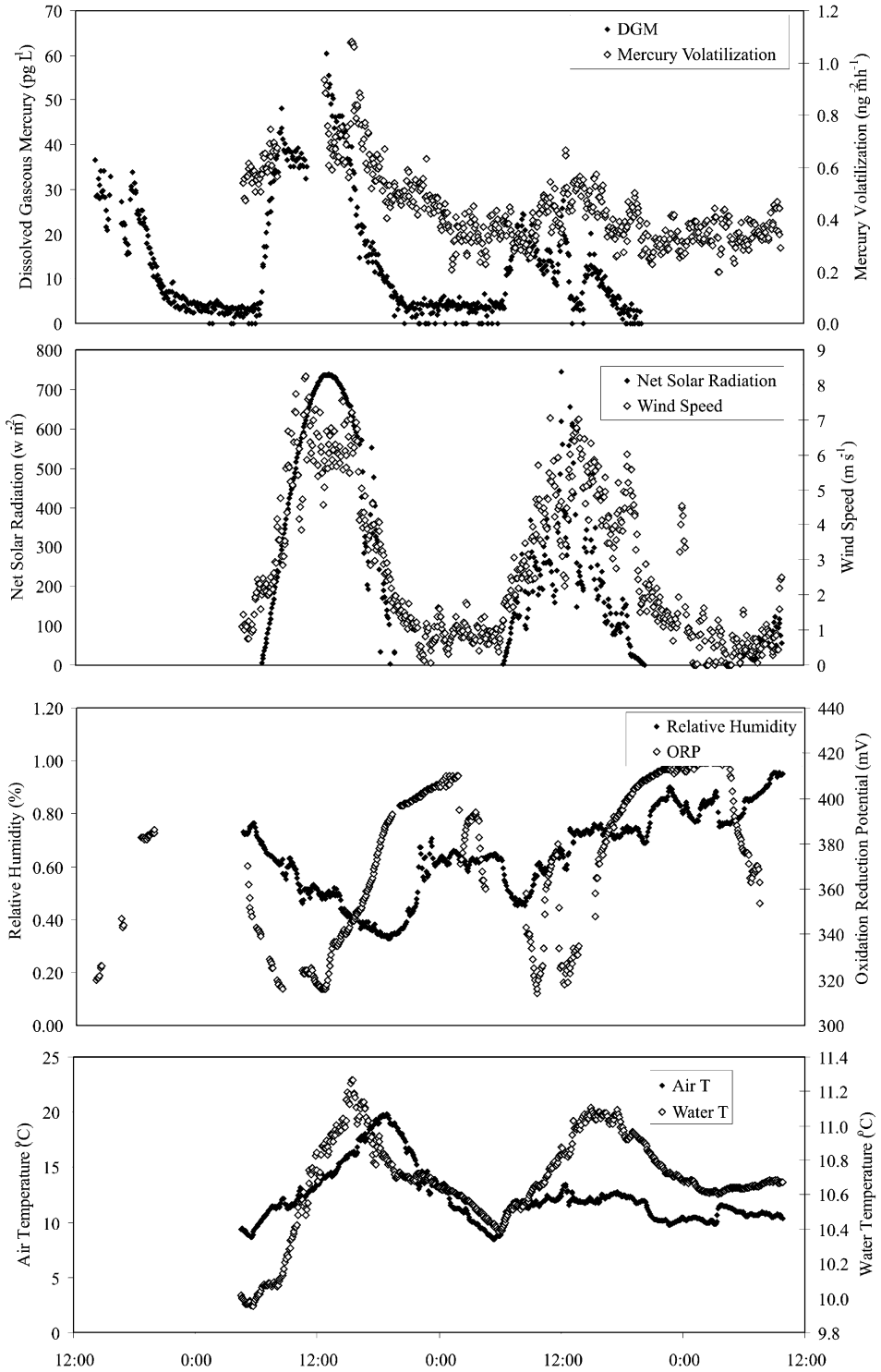


**FIGURE 1. Diurnal patterns observed in DGM, mercury volatilization, net solar radiation, wind speed, relative humidity, oxidation reduction potential, water temperature, and air temperature in the St. Lawrence River.**

As shown in Figure 2, the highest correlation between DGM concentrations and mercury volatilization occurred with a lag-time of 135 min (correlation = 0.625). Taking into account the standard error on the correlation maximum (0.05) the likely lag-time ranged between 55 and 145 min (corresponding correlation of 0.578−0.599). This indicates a lag-time of 55−145 min between DGM formation and its subsequent volatilization from the water surface. This measured lag-time matches well with estimated surface water Eddy diffusion times of 42−132 min (for a mixed layer depth of 5−7.5 m) measured in the St. Lawrence River (*27*) and suggests that diffusion of DGM in the water column may partially control the extent of the lag-time. Lag-times of up to 1 h have been observed between mercury flux and water temperature in the Bay Saint Francois wetlands on the St. Lawrence River (*28*). This also may suggest a lag-time between solar induced DGM formation and mercury volatilization in Bay Saint Francois. In addition to water eddy diffusion times, it is likely that turbulent transfer velocity between air and water may also affect the lag time between DGM formation and mercury volatilization. The most accurate method to incorporate wind speed in mercury volatilization models is still a subject of much debate. Incorporation of wind speed has been shown to result in increased variability in model

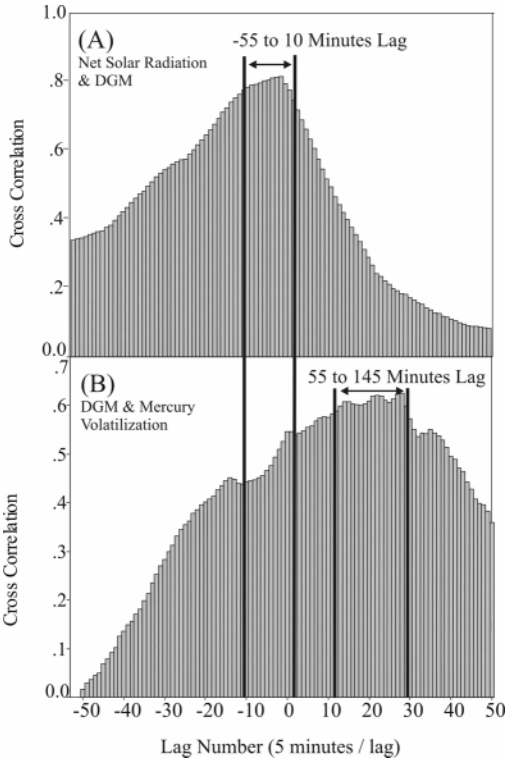


**FIGURE 2. Cross-correlation coefficient versus lag number (5 min/lag) for (A) net solar radiation and DGM concentration, and (B) DGM and mercury volatilization.**

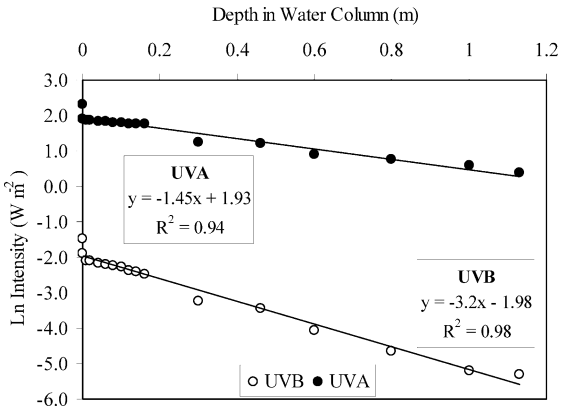


**FIGURE 3. Depth in the St. Lawrence River water column versus the natural logarithm of intensity for UVB and UVA radiation. The negative slope of the linear regression for each curve equals the diffuse integrated attenuation coefficient ($K_{dI\ UVB}$ and $K_{dI\ UVA}$).**

predictions in comparison to quantitative data (*13*), recent work examining flux model development has confirmed this observation (*28*).

**Attenuation of Ultraviolet Radiation with Depth.** The total cumulative UVB radiation received by the St. Lawrence River on days 1 and 2 of the experiment was 150 kJ $m^{-2}$ and 73 kJ $m^{-2}$ respectively. The total cumulative UVA radiation received by the St. Lawrence River on days 1 and 2 of the experiment was 2777 kJ $m^{-2}$ and 1362 kJ $m^{-2}$ respectively. We observed that 26% total incoming UVB and 52% of total incoming UVA radiation was available at a depth of 0.3 m (Figure 3). The diffuse integrated vertical attenuation coefficients for UVB and UVA radiation ($K_{dI\ UVA}$ = 1.45 $m^{-1}$ and $K_{dI\ UVB}$ = 3.20 $m^{-1}$) were calculated using the method outlined by Scully and Lean (*21*).

Many researchers have identified DOC and total suspended solids (TSS) as the principal attenuators of solar radiation in most freshwaters (*21*, *29*−*32*). As such, the low rates of UV attenuation observed in the St. Lawrence River can likely be attributed to low concentrations of both dissolved organic carbon (mean = 2.58 mg $L^{-1}$; SD = 0.15; $n$ = 24) and TSS (mean = 0.58 mg $L^{-1}$; SD = 0.39; $n$ = 5) in the St. Lawrence River during the analysis. The low TSS concentration in the St. Lawrence River is likely a result of low productivity (midsummer chlorophyll is typically <1 $\mu$g $L^{-1}$) and the fact that the river's headwaters are Lake Ontario, which is a large settling basin for particulates (*33*).

**Near-Sediment DGM Concentrations.** Siciliano et al. (*9*) observed increases in DGM concentration when approaching the sediment water interface in Lake Ontario. To test for similar results in the St. Lawrence River DGM concentrations were measured in near sediment water (2−3 cm above the sediment surface at an approximate depth of 1.5 meters) over a 12 h period (20:00−10:00). DGM concentrations were found to be similar to night-time DGM values in surface water (ranging from 0 to 5.7 pg $L^{-1}$, $n$ = 167) and did not increase significantly with increases in incoming net solar radiation (see Supporting Information; Figure SI-2). As previously noted, ultraviolet radiation (280−400 wavelength range) was mostly attenuated by 1 m depth (>96% UVB and >73% UVA attenuation).

Since DGM concentrations near sediment were negligible and unchanging it was concluded that there was no near-sediment production of DGM. These results suggest that DGM production in the St. Lawrence River is primarily via photoinduced reduction mechanisms. While photoinduced biological reduction has also been observed (*6*), the relative importance of the photobiological pathway was not assessed here. Amyot et al. (*10*) did not observe any difference in DGM production between filtered and nonfiltered St. Lawrence River samples indicating that abiotic photochemical reduction is likely the primary pathway of DGM formation in the St. Lawrence River.

**Modeling DGM Formation with Depth.** A linear regression of net radiation versus DGM concentration (eq 3) was found to fit the data well ($r^2$ = 0.62; $p$ < 0.001).

$$DGM_t = 0.032 \bullet I_{0NET} + 4.949 \quad (3)$$

Where: $DGM_t$ = dissolved gaseous mercury in pg $L^{-1}$ at time $t$; $I_{0\ NET}$ = net incoming radiation intensity (W $m^{-2}$) at time $t$

However, several researchers have observed that UV radiation is principally responsible for DGM production in freshwaters (*5*, *8*). O'Driscoll et al. (*8*) found that UVA and UVB radiation are equally important in determining gross DGM production kinetics in similar freshwater systems (e.g., lakes or rivers); however, rates of photooxidation were not assessed. Unpublished data from O'Driscoll et al. (*8*) found that exposure of freshwaters to PAR radiation did not result in significant mercury reduction (See Supporting Information Figures SI-3 and SI-4). We would note that while this data (Figures SI-3 and SI-4) suggests that visible radiation may be of minor importance in mercury reduction kinetics, more research is required to confirm these results. In addition, Garcia et al. (*7*) found that UVB radiation was more important to net DGM production in low DOC freshwaters (such as the St. Lawrence River) than was UVA radiation. In the work presented here, a model was derived based on UVB radiation. A constant proportion of UVB radiation for this longitude (0.7% of net radiation, SB = 0.4) was calculated based on $n$ = 234 readings in Central Quebec (*26*) and confirmed with several spectral scans of incoming radiation during this experiment. Similar to net radiation, a linear regression of net UVB radiation versus DGM concentration (eq 4) was found to fit the data well ($r^2$ = 0.62; $p$ < 0.001). Since no lag-time was observed between net radiation and DGM

concentrations in surface water a lag-time correction was not incorporated in this model as was required for previous DGM models for freshwater lakes (*13*).

$$DGM_t = 4.625 \bullet I_{0UVB} + 4.949 \quad (4)$$

Where: $DGM_t$ = dissolved gaseous mercury in pg $L^{-1}$ (or ng $m^{-3}$) at time *t*; $I_{0UVB} = I_{0NET} \times 0.007$

Therefore by using the linear regression model (eq 4) and incorporating Beers law (eq 2) to account for the attenuation of UVB radiation with depth, we can calculate the depth-integrated areal DGM concentration at any solar radiation intensity (eq 5).

$$DGM_{areal} = \int_{z_2}^{z_1} [4.625 \bullet (I_{0UVB} e^{-K_{dIUVB} \bullet Z}) + 4.949] \quad (5)$$

Where: $DGM_{areal}$ is dissolved gaseous mercury on an areal basis in the integrated water column (pg $m^{-2}$) at time *t*; $\int_{z_2}^{z_1}$ is The integral between $z_1$ and $z_2$ depth (m) in the water column (e.g., for total water column at site $z_1 = 0$ and $z_2 =$ 1.3 m); $I_{0UVB} = I_{0NET} \cdot 0.007$; $I_{0\ NET}$ is net incoming radiation at time *t*; $K_{dIUVB}$ is the diffuse integrated attenuation coefficient for UVB radiation (3.20 $m^{-1}$); and $z$ = depth in meters.

The techniques used to create this model can be used in a variety of ecosystems to determine the general applicability of this model to a variety of aquatic systems. The current model calculations are based on a 3 day sampling period and it should be noted that $K_{dIUVB}$ values may change seasonally and spatially within the St. Lawrence River.

Equation 5 was solved using the Simpson algorithm in MATLAB (release 14) software to determine the depth-integrated areal concentrations for several different portions of the water column (e.g., 0−1.3 m and 0−0.30 m depth). It was observed that only 26% of DGM in the total water column was produced in the top 0.3 m (i.e., 74% of DGM is produced at depths >0.3 m). This production of DGM at depth combined with diffusion and mixing processes in the St. Lawrence River likely explains the homogeneous distribution of DGM with depth observed by Amyot et al. (*10*). In contrast, dynamic changes in DGM concentration with depth have been measured in stratified lakes containing higher concentrations of DOC (*9*, *10*).

Areal concentrations will change not only spatially but also temporally with changes in solar radiation. Areal concentrations for our site (0−1.3 m depth) ranged between 6.4 to 13.8 ng $m^{-2}$ during the 68 h sampling period. While these results are the first areal DGM concentrations examined over a full photoperiod, we can compare to the few published areal DGM concentrations available. For example, Siciliano et al., (*9*) used DGM depth profiles to calculate areal concentrations of DGM approximately at midday ranging between 94 and 850 ng $m^{-2}$ (9−18 m depth) in Jack's Lake, Ontario (unit correction from Siciliano, personal communication). In addition, areal DGM measurements for Lake Ontario sites sampled at various times of day ranged between 0 and 13 000 ng $m^{-2}$ for 27−210 m depth. The average DGM in each whole lake system, derived from the depth integrated DGM values, is reasonably similar between the three freshwaters (ranging from 0 to 61 ng $m^{-3}$ or 0 to 61 pg $L^{-1}$).

The depth-integrated DGM model developed found that the top 0.3 m of the water column accounted for only 26% of the total depth-integrated DGM. A comparison with volatilization data indicated that a large portion (76% or 10.5 ng $m^{-2}$) of the maximum depth-integrated DGM (13.8 ng $m^{-2}$) is volatilized over a 24-hour period. Therefore at least 50% of all DGM volatilized was produced at depths below 0.3 m. Therefore the Eddy diffusion of DGM from deeper in the water column to the surface is a probable explanation for the lag-time observed between DGM formation and mercury volatilization. As previously noted the 55−145 min lag-time observed between DGM formation and volatilization matches very well with estimated surface water (5−7.5 m) Eddy diffusion times (42−132 min) in the St Lawrence River (*27*).

These results highlight the importance of solar attenuation in regulating DGM formation with depth. These results also demonstrate both the fast formation of DGM in rivers and the importance of DGM distribution with depth in determining mercury volatilization dynamics. Given diffuse vertical attenuation coefficients over a spatial and temporal basis and bathymetric readings for the St. Lawrence River, the depth-integrated DGM model derived here could be used to calculate areal DGM production over the entire river on a seasonal basis. Using the techniques presented here, similar models may be derived for other freshwaters that will provide a major advantage over the current surface water based DGM models.

## Acknowledgments

This research was supported by an NSERC strategic grant to David Lean and NSERC postdoctoral fellowship to Nelson O'Driscoll. The St. Lawrence River Institute and Environment Canada (Centre St. Laurent) provided additional funding and field support. Thanks to Tania Delongchamp (University of Ottawa), Martin Pilote (Environment Canada), and the technicians at the St. Lawrence River Institute for field and technical support. Thanks to Derek Mueller (University of Alaska) for MATLAB program for integral analysis.

## Supporting Information Available

(i) Site location map; (ii) graph of near sediment DGM readings in comparison to surface water; (iii) two graphs showing unpublished data for DGM formation by visible radiation in two freshwater systems. This material is available free of charge via the Internet at http://pubs.acs.org.

## Literature Cited

(1) O'Driscoll, N. J.; Beauchamp, S.; Clair, T. A; Rencz, A. N.; Telmer, K.; Siciliano, S. D; Lean, D. R. S. Chapter 13: A mercury mass balance for Big Dam West Lake: Examining the role of volatilisation. In *Mercury Cycling in a Wetland Dominated Ecosystem: A Multidisciplinary Study*; O'Driscoll, N. J., Rencz, A. N., Lean, D. R. S., Eds.; SETAC Publishers: Lawrence, KS, 2005.

(2) Orihel, D. M.; Paterson, M. J.; Gilmore, C. C.; Bodaly, R. A.; Blanchfield, P. J.; Hintelmann, H.; Harris, R. C.; Rudd, J. W. M. Effect of loadingrate on the fate of mercury in littoral mesocosms. *Environ. Sci. Technol.* **2006**, *40* (19), 5992−6000.

(3) Poulain, A. J.; Orihel, D. M.; Amyot, M.; Paterson, M. J.; Hintelmann, H.; Southworth, G. R. Relationship between the loading rate of inorganic mercury to aquatic ecosystems and dissolved gaseous mercury production and evasion. *Chemosphere*. **2006**, *65*, 2199−2207.

(4) Gao, N.; Armatas, N. G.; Shanley, J. B.; Kamman, N. C.; Miller, E. K.; Keeler, G. J.; Scherbatskoy, T.; Holsen, T. M.; Young, T.; Mcilroy, L.; Drake, S.; Olsen, B.; Cady, C. Mass balance assessment for mercury in Lake Champlain. *Environ. Sci. Technol.* **2006**, *40*, 82−89.

(5) Amyot, M.; Mierle, G.; Lean, D.; McQueen, D. Effect of solar radiation on the formation of dissolved gaseous mercury in temperate lakes. *Geochem. Cosmochem. Acta*. **1997**, *61* (5), 975−987.

(6) Siciliano, S. D.; O'Driscoll, N. J.; Lean, D. R. S. Microbial reduction and oxidation of mercury in freshwater lakes. *Environ. Sci. Technol.* **2002**, *36*, 3064−3068.

(7) Garcia, E.; Amyot, M.; Ariya, P. A. Relationship between DOC photochemistry and mercury redox transformations in temperate lakes and wetlands. *Geochim. Cosmochim. Acta* **2005**, *69* (8), 1917−1924.

(8) O'Driscoll, N. J.; Siciliano, S. D.; Lean, D. R. S.; Amyot, M. Gross photo-reduction kinetics of mercury in temperate freshwater lakes and rivers: Application to a general model for DGM dynamics. *Environ. Sci. Technol.* **2006**, *40*, 837−843.

(9) Siciliano, S. D.; O'Driscoll, N. J.; Lean, D. R. S. Dissolved gaseous mercury profiles in freshwaters. In *Biogeochemistry of Envi-*

*ronmentally Important Trace Elements*; Cai, Y., Braids, O. C., Eds.; ACS Symposium Series 835; American Chemical Society: Washington, DC, 2002.
(10) Amyot, M.; Lean, D. R. S.; Poissant, L.; Doyon, M. Distribution and transformation of elemental mercury in the St. Lawrence River and Lake Ontario. *Can. J. Fish. Aquat. Sci.* **2000**, *57* (Suppl. 1), 155−163.
(11) Poulain, A. J.; Amyot, M.; Findlay, D.; Telor, S.; Barkay, T.; Hintelmann, H. Biological and photochemical production of dissolved gaseous mercury in a boreal lake. *Limnol. Oceanog.* **2004**, *49* (6), 2265−2275.
(12) O'Driscoll, N. J.; Rencz, A. N.; Lean, D. R. S. Chapter 14: The biogeochemistry and fate of mercury in natural environments. In *Metal Ions in Biological Systems*; Sigel, A., Sigel, H., Sigel, R.K.O., Eds.; Marcel Dekker, Inc.: New York, 2005; Vol. 43.
(13) O'Driscoll, N. J.; Beauchamp, S.; Siciliano, S. D.; Rencz, A. N.; Lean, D. R. S. Continuous analysis of dissolved gaseous mercury (DGM) and mercury flux in two freshwater lakes in Kejimkujik Park, Nova Scotia: Examining flux models with quantitative data. *Environ. Sci. Technol.* **2003**, *37* (10), 2226−2235.
(14) Poissant, L.; Casmir, A. Water-air and soil-air exchange rate of total gaseous mercury measured at background sites. *Atmos. Env.* **1998**, *32* (5), 883−893.
(15) Poissant, L.; Pilote, M.; Casimir, A. Mercury flux measurements in a naturally enriched area: correlation with environmental conditions during the nevada SToRMS (Nevada study and tests of the release of mercury from soils). *J. Geophys. Res.* **1999**, *104* (D17), 21845−21857.
(16) Poissant, L.; Pilote, M.; Constant, P.; Beauvais, C.; Zhang, H.; Xu, X. Mercury gas exchanges over selected bare soil and flooded sites in the Bay St. François Wetlands (Québec, Canada). *Atmos. Env.* **2004**, *38*, 4205−4214.
(17) Gustin, M. S.; Casimir, A.; Ebinghaus, R.; Edwards, G.; Fitzgerald, C.; Kemp, J.; Kock, H. H.; Lindberg, S. E.; London, J.; Majewski, M.; Marsik, F.; Owens, J.; Poissant, L.; Pilote, M.; Rasmussen, P.; Schaedlich, F.; Schneeberger, D.; Sommer, J.; Turner, R.; Vette, A.; Washlager, D.; Xiao, Z. The desert StoRMS project: Intercomparison of mercury fluxes measured in situ with seven field chambers and four micrometeorological methods, Stemboat Springs, Nevada. *J. Geophys. Res.* **1999**, *104* (D17), 21831−21844.
(18) Xiao, Z. F.; Munthe, J.; Schroeder, W. H.; Lindqvist, O. Vertical fluxes of volatile mercury over forest soil and lake surfaces in Sweden. *Tellus* **1991**, *43B*, 267.
(19) Morin, J.; Leclerc, M. From pristine to present state: Hydrology evolution of Lake St. Francis, St. Lawrence River. *Can. J. Civ. Eng.* **1998**, *25*, 864−879.
(20) O'Driscoll, N. J.; Siciliano, S.; Lean, D. R. S. Continuous analysis of dissolved gaseous mercury in freshwater ecosystems. *Sci. Total Environ.* **2003**, *304* (1−3), 285−294.
(21) Scully, N. M.; Lean, D. R. S. The attenuation of ultraviolet radiation in temperate lakes. *Arch. Hydrobiol. Beih. Ergebn. Limnol.* **1994**, *43*, 135−144.
(22) Hall, G. E. M.; Pelchat, J. C.; Pelchat, P.; Vaive, J. E. Sample collection, filtration and preservation protocols for the determination of 'total dissolved' mercury in waters. *The Analyst* **2002**, *127*, 674−680.
(23) United States Environmental Protection Agency. *Method 1631, Revision E: Mercury in Water by Oxidation, Purge and Trap, and Cold Vapor Atomic Fluorescence Spectrometry*; EPA-821-R-02-01; U.S. EPA: Washington, DC, 2002.
(24) Poissant, L.; Amyot, M.; Pilote, M.; Lean, D. Mercury water - Air exchange over the upper St. Lawrence River and Lake Ontario. *Environ. Sci. Technol.* **2000**, *34* (15), 3069−3078.
(25) O'Driscoll, N. J.; Siciliano, S. D.; Peak, D.; Carignan, R.; Lean, D. R. S. The influence of forestry activity on the structure of dissolved organic matter in lakes: Implications for mercury photo-reactions. *Sci. Total Env.* **2006**, *366*, 880−893.
(26) O'Driscoll, N. J.; Lean, D. R. S.; Loseto, L.; Carignan, R.; Siciliano, S. D. The effect of dissolved organic carbon on the photoproduction of dissolved gaseous mercury in lakes and the potential impacts of forestry. *Environ. Sci. Technol.* **2004**, *38*, 2664−2672.
(27) Scully, N. M.; Vincent, W. F.; Lean, D. R. S. Exposure to ultraviolet radiation in aquatic ecosystems: estimates of mixing rate in Lake Ontario and the St. Lawrence River. *Can. J. Fish. Aquat. Sci.* **2000**, *57* (Suppl. 1), 43−51.
(28) Zhang, H. H.; Poissant, L.; Xu, X.; Pilote, M.; Beauvais, C.; Amyot, M.; Garcia, E.; Laroulandie, J. Air-water gas exchange of mercury in the Bay Saint François wetlands: Observation and model parameterization. *J. Geophys. Res.* **2006**, *111* (D17), doi:10.1029/2005JD006930.
(29) Morris, D. P.; Zagarese, H.; Williamson, C. E.; Balseiro, E. G.; Hargreaves, B. R.; Modenutti, B.; Moeller, R.; Queimalinos, C. The attenuation of solar UV radiation in lakes and the role of dissolved organic carbon. *Limnol. Oceanog.* **1995**, *40* (8), 1381−1391.
(30) Morris, D. P.; Hargreaves, B. R. The role of photochemical degradation of dissolved organic carbon in regulating the UV transparency of three lakes on the pocono plateau. *Limnol. Oceanog.* **1997**, *42* (2), 239−249.
(31) Smith, R. E. H.; Furgal, J. A.; Charlton, M. N.; Greenberg, B. M.; Hiriart, V.; Marwood, C. Attenuation of ultraviolet radiation in a large lake with low dissolved organic matter concentrations. *J. Fish. Aquat. Sci.* **1999**, *56* (8), 1351−1361.
(32) Maloney, K. O.; Morris, D. P.; Moses, C. O.; Osburn, C. L. The role of iron and dissolved organic carbon in the absorption of ultraviolet radiation in humic lake water. *Biogeochemistry.* **2005**, *75* (3), 393−407.
(33) Ridal, J.; Doran, B.; Nwobu, O.; Lean, D. R. S. *Assessment of Mercury Concentrations in Zooplankton Populations in the Zones of Contaminated Sediments and Comparison to Reference Sites in the St. Lawrence River (Cornwall) Area of Concern*; Report to the Ontario Ministry of the Environment: Toronto, 2006.

*Received for review January 19, 2007. Revised manuscript received May 3, 2007. Accepted May 9, 2007.*

ES070147R